CERN 78-03
Experimental Physics
Facilities Division
13 March 1978

ORGANISATION EUROPÉENNE POUR LA RECHERCHE NUCLÉAIRE
CERN EUROPEAN ORGANIZATION FOR NUCLEAR RESEARCH

DESIGN AND CONSTRUCTION OF TWO 10.8 T·m SUPERCONDUCTING BEAM BENDING MAGNETS

P. Dow and G. Kesseler

G E N E V A

1978

CERN - Service d'information scientifique - RD/313 - 2000 - mars 1978

ABSTRACT

Constructional details are given of two superconducting beam bending magnets built at CERN in 1975-77. Each magnet unit has a bending power of 10.8 T·m at the nominal current of 700 A, corresponding to a central induction of 4.75 T in a cold bore of 74 mm diameter. An 'intersecting-ellipses' coil configuration is approximated by 36 horizontally wound racetrack layers of rectangular cross-section with 90° bends at the coil ends. A cold-iron magnetic shield serves, in addition, as retaining structure for the electromagnetic forces. The vacuum-insulated liquid helium vessel is surrounded by a radiation shield cooled by helium boil-off gas and supported by a fibre-glass/stainless steel suspension system. The cryogenic losses of each magnet cryostat are approximately 4 W excluding transfer losses. After successful tests the magnets were placed in a particle beam where they have been regularly operated on automatic control for about one year.

CONTENTS

1. INTRODUCTION

A group of three superconducting beam bending magnets, providing a maximum bending power of 27 T•m, has been installed in the hadron (s_3) beam to the Big European Bubble Chamber (BEBC), at CERN.

The three magnet units, called SBM I, II, and III in the sequence of their construction, are arranged as shown schematically in Fig. 1. Magnet I is an older-type magnet which was formerly used in the u_7 beam[1]. The magnet units II and III, more recently constructed and of improved design, are identical to each other.

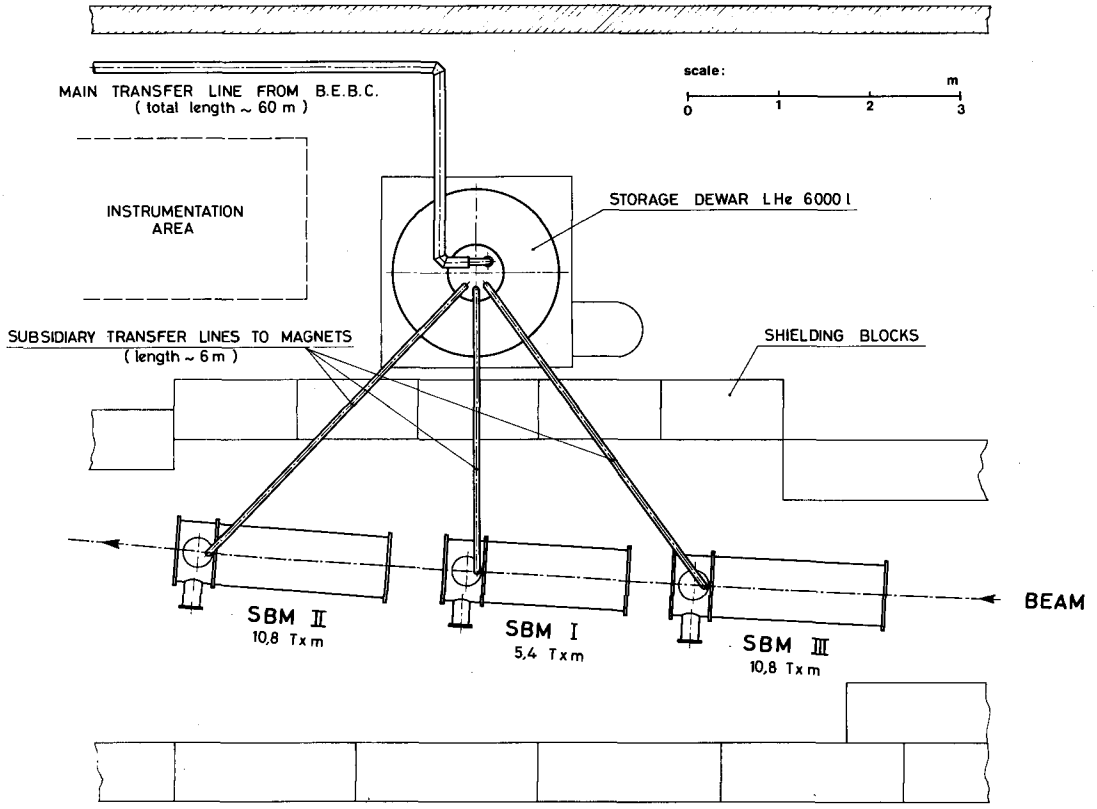

Fig. 1 Arrangement of magnets in beam line

Liquid helium is transferred to the three magnets from a 6,000 litre storage dewar, which is periodically filled by means of a 60 m long transfer line, connected to the liquefaction plant of BEBC. The power supply and all instrumentation necessary for the magnet control are placed outside the beam shielding near to the dewar. During one year of operation, the system has proved to work fully automatically with a high degree of reliability and a minimum of supervision.

This report will describe the design, the manufacture, and some operational results of the magnet units II and III. A description of the installation in the beam area, including the liquid helium transfer and storage system, will be given in a separate paper.

2. GENERAL

The beam bending angle of 54 mrad and the maximum beam momentum of 150 GeV/c require a total bending power of 27 T•m at the bending point in question. The already existing superconducting magnet SBM I could provide 5.4 T•m. The remaining 21.6 T•m are supplied by the two identical units SBM II and III to be described in this paper.

An alternative solution would have been to construct a single, longer magnet unit to produce the whole of the required bending power; however, this was found unfavourable mainly for the following reasons:

i) as the aperture becomes greater owing to the increased sagitta on the curved beam path within the magnet, the cost per metre of magnet length goes up considerably;

ii) existing equipment for winding, assembly, and testing could be used (with minor changes) for a magnet length of up to about 3 m;

iii) with two further units a symmetric set-up was possible, allowing the central magnet (SBM I) to be switched off at beam momenta below 120 GeV/c without any change in the beam geometry.

The design of the cryostats of magnets SBM II and III was largely influenced by the experience already gained with SBM I. In contrast, however, the coil design is considerably different. SBM I has an entirely epoxy impregnated coil and, when initially charged, required a high number of training quenches before approaching its design current. The idea behind the design of the new magnets was to allow some liquid helium to be in close contact with the conductor inside the coil. Although the advantage of good cooling is not evident for intrinsically stable superconductors, many practical examples have shown that magnets, when initially charged, perform better (i.e. show less training) when the cooling is improved.

This observation is particularly true for transverse field magnets such as dipoles, in which the direction of the electromagnetic forces is perpendicular to the conductor and must be entirely taken up by mechanical structures surrounding the coil. In the past, a number of such magnets have shown excessive training. Whatever the reasons for the training[2], it is certain that small amounts of energy are released during the charging cycle of such a magnet. Whether or not a local energy burst is sufficient to trigger a quench, depends on the cooling which, in turn, can be considerably improved by the presence of liquid helium.

Three more practical aspects were also considered when fixing the design parameters:

i) a "cold bore", i.e. a common vacuum for the cryogenic insulation and for the beam passage, seemed to be the simplest and cheapest solution for a bending magnet;

ii) the same type of superconductor as used for SBM I had to be considered for the new magnets, since some lengths were still in stock;

iii) the nominal current could be the same for all three magnets to allow for series operation, thereby making economic use of the existing highly stabilized power supply.

Table 1 gives some of the main parameters of the magnets.

Table 1

Magnet parameters (per unit)

Bending power	max. 10.8 T•m
Bending field	max. 4.75 T
Peak field in winding	approx. 5.2 T
Inhomogeneity of field integral	max. 4×10^{-3}
Nominal current	700 A
Stored energy	0.32 MJ
Aperture (cold bore)	74 mm
Inner diameter of iron	200 mm
Outer diameter of iron	400 mm
Magnetic length	2.28 m
Physical length of coil	2.43 m

3. MAGNET DESIGN AND ASSEMBLY

3.1 Conductors

The conductors used for SBM II and III are somewhat different in composition, but the design of both is based on the same over-all size and critical current (Table 2).

Each magnet required 4800 metres of composite conductor. A few short samples from this length were tested, and the critical current was always found to be in accordance with the specification.

Table 2

Superconductor parameters

	Conductor used for		Specification
	SBM II	SBM III	
Size incl. insulation (mm × mm)	Within specificat.		$1.5^{+0}_{-0.1} \times 3^{-0.1}_{-0.15}$
Cu/SC ratio	1.25	2.5	Not spec.
No. of filaments	367	567	Not spec.
Twist pitch (mm)	25	30	Max. 30
Average filament diameter (μm)	80	50	Not spec.
Critical current (typical)			
at 5 T (A)	1500	1500	Min. 1250
at 6 T (A)	1200	1200	Min. 1000
at 7 T (A)	Not tested	900	Not spec.

The operating point on the load line (Fig. 2) was placed at 80% of the distance between the origin and the intersecting point with the specified critical current curve. The resulting safety margin seemed to be adequate in view of the fairly low copper-to-superconductor ratio of the conductor used for SBM II. The over-all current density in the winding is 156 A/mm^2 at nominal current.

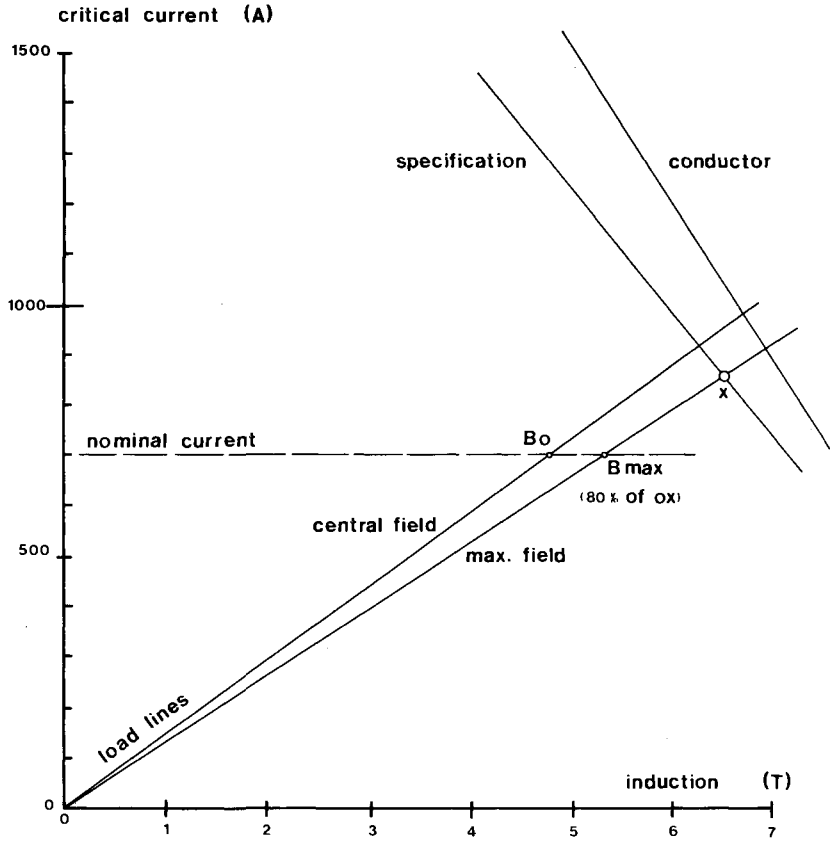

Fig. 2 Critical current -- field characteristics of composite conductors with magnet load lines

3.2 Coil geometry

Good experience has been gained in the past with horizontally wound "racetrack" coils. Desportes[3] summarized the advantages of this winding configuration, and his results were confirmed with these magnets.

A cut through the straight section of the magnet is shown in Fig. 3a. The ends of the racetrack coils are bent up by 90° as can be seen in Fig. 3b. All the layers were wound separately and connected in series by means of indium-soldered joints immersed in the liquid helium.

The field calculations were first made for the two-dimensional case with the MAGNET program[4], which allows for saturation effects in the iron. When a satisfying coil geometry had been found, a half magnet was computed using the three-dimensional program MAG 4 [5] with one coil end included. Although the coil end geometry had to be simplified to reduce the

data input, the results of this calculation proved that the geometry of the coil was acceptable. Excellent agreement was found between both programs in the region where both are valid, i.e. in the straight part of the magnet.

From the calculations it followed that the field inhomogeneities depend on the field level because of saturation effects in the iron which, in turn, can be influenced by the iron shield thickness. The latter was chosen in such a way that the field distortion did not exceed 4×10^{-3} at the nominal current and was less at lower currents.

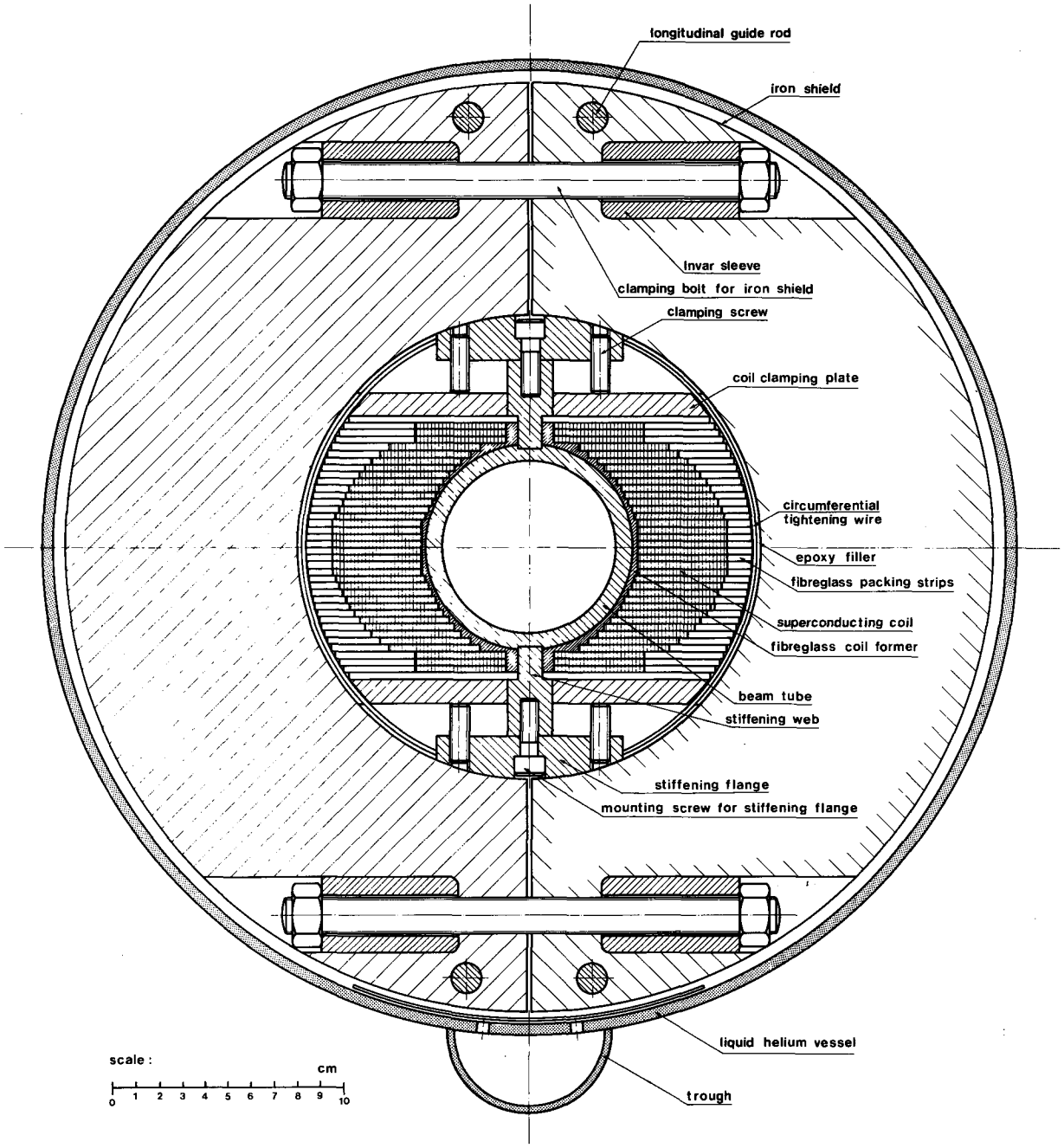

Fig. 3a Typical cross-section through straight part of magnet

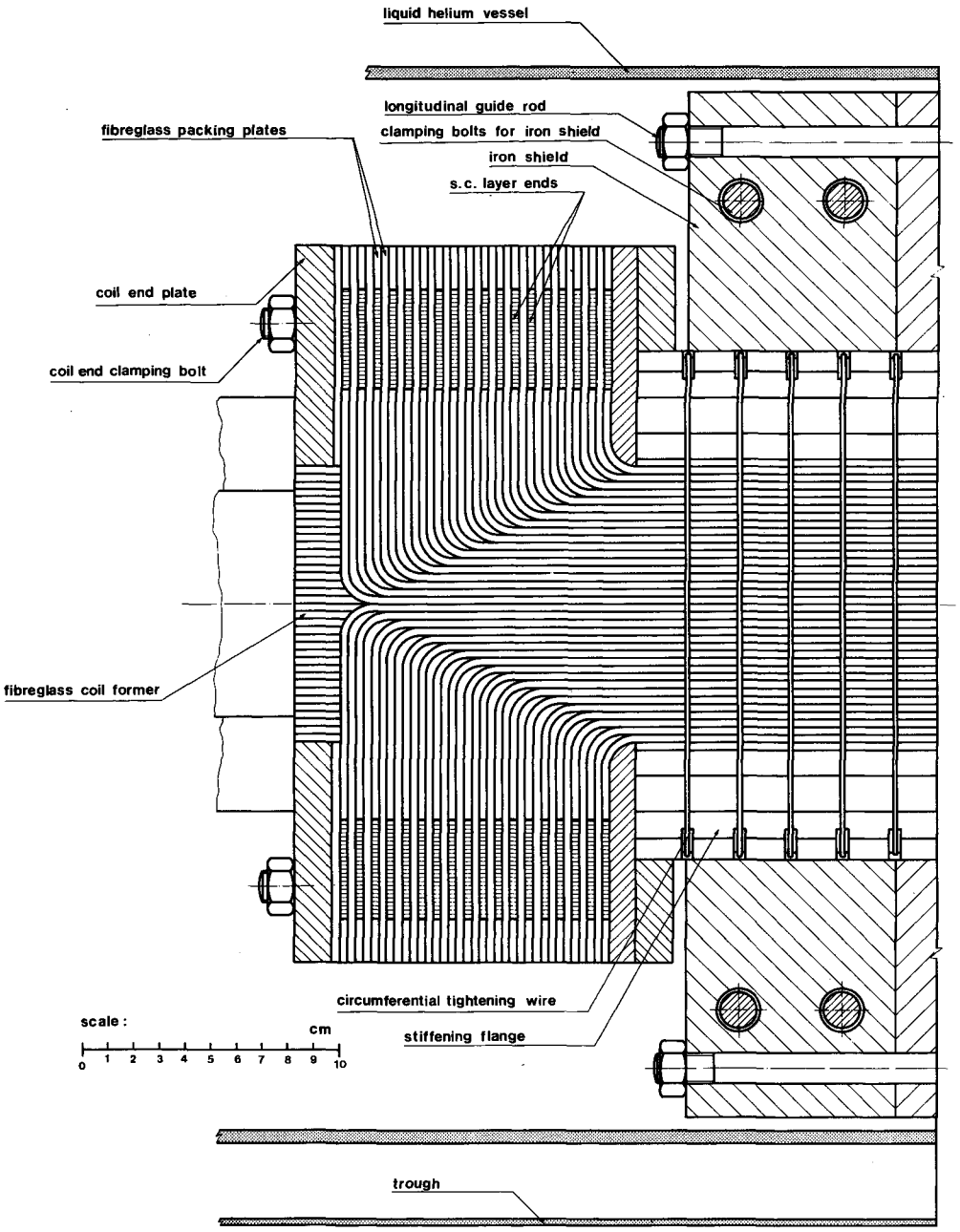

Fig. 3b Longitudinal section through coil end

3.3 Coil winding

Winding of the coil layers was performed on a horizontal winding table around suitable forms (Fig. 4). The wire orientation was such that the rectangular cross-section stood upright, and the tension on the conductor was kept at approximately 2.5 kg/mm^2. When the layer (each layer consisting of 26 turns) was finished, an extension piece at each end of the table was removed, so that the end of the layer could be bent down as a whole (Figs. 5 and 6). Since the superconductor is fairly springy, the bending angle, defined by an adjustable stop, had to be somewhat greater than the 90° required by the coil geometry.

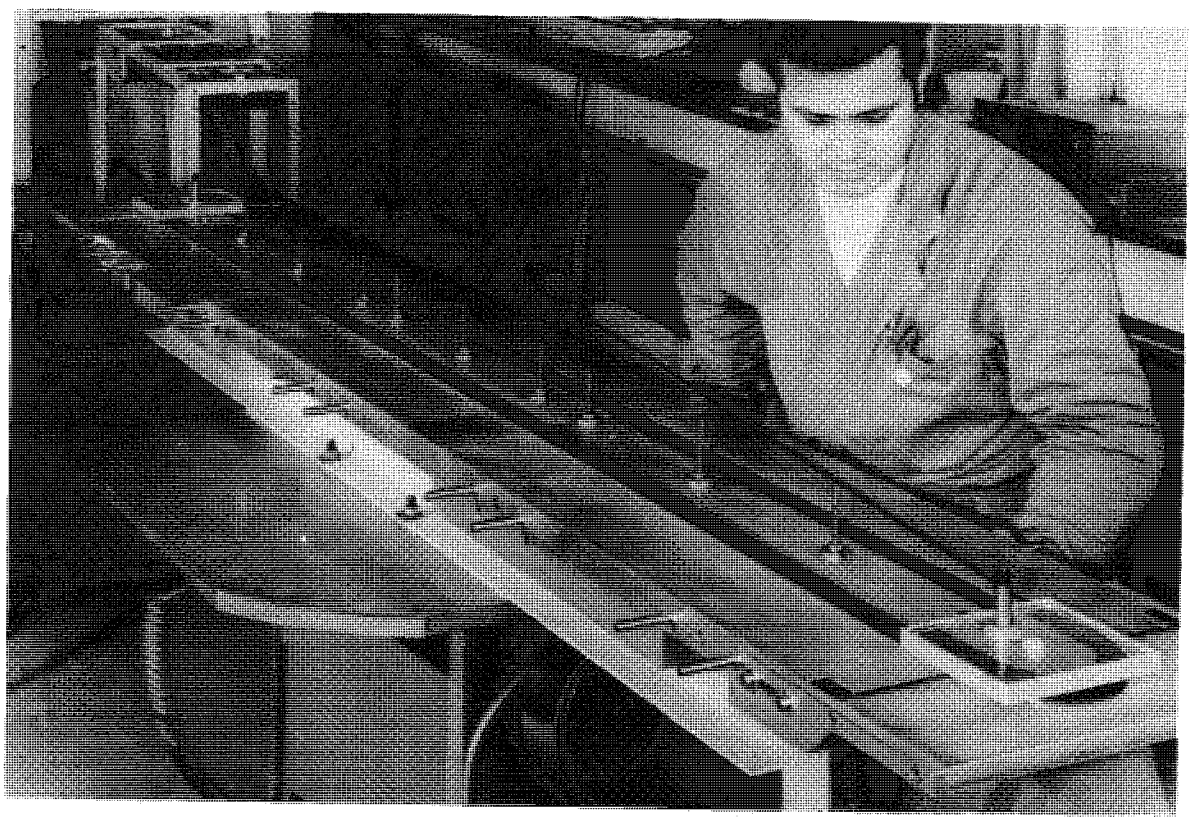

Fig. 4 Winding table

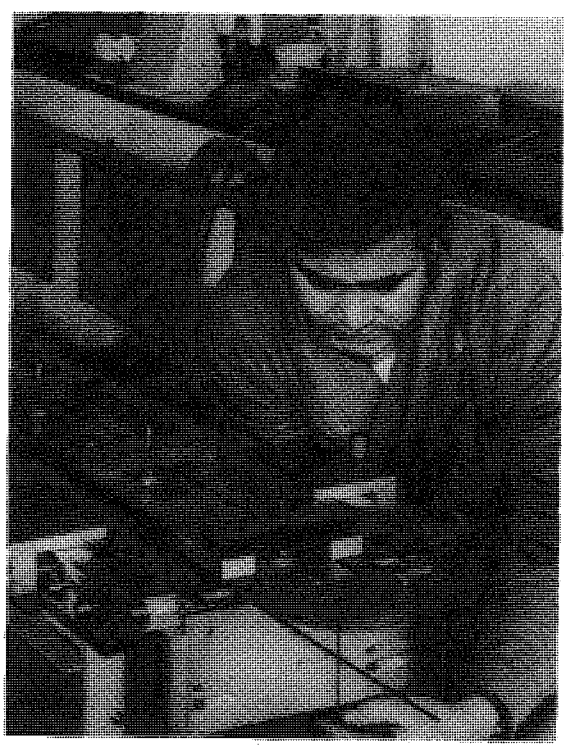

Fig. 5 Winding table with extension piece removed prior to bending of coil end

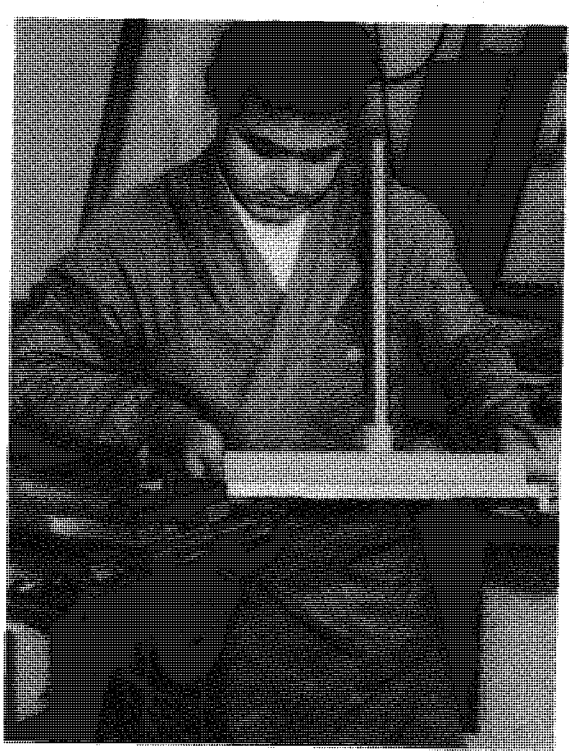

Fig. 6 Winding table with coil end bent down

In spite of the earlier remark concerning epoxy resin in the winding, it was found necessary to use a small amount in order to keep the layers in shape. The quantity, however, was small, about 5 g for a whole layer.

Since the behaviour of several different epoxy mixtures had already been studied at low temperatures, we selected one which seemed to be the most favourable, namely No. 79 in the publication of D. Evans et al.[6], the composition of which is given in Table 3. Curing was performed at approx. 75°C for about 12 hours with the layer clamped tightly to the table and the winding formers.

Table 3

Epoxy resin composition

MY 740 (Ciba)	60 pbw
CY 208 (Ciba)	40 pbw
D 230 (Jefferson)	35 pbw

Each layer was tested against inter-layer shorts by measuring the resonance curve of a resonant circuit formed by the layer as self-inductance and a capacitor of 470 pF. Out of the whole 72 layers needed for the two magnets, one had to be eliminated because of an internal short circuit.

The mechanical dimensions of the finished layers were also checked and were found to be within the required tolerances.

3.4 Coil assembly

The central part of the magnet (Fig. 3a) consists of a stainless steel beam tube, the bore of which forms the beam path. Since the beam tube carries the whole load of the coil and the iron (approx. 1750 kg), and is supported only at its ends, it had to be stiffened by adding the two sections called "stiffening web" and "stiffening flange". The two curved stiffening flanges also serve as a location for the magnetic iron with respect to the horizontal magnet symmetry plane. Two fibre-glass half shells were glued on either side of the beam tube and then machined precisely to the inner shape of the coil, referred to as "coil former" in Fig. 3a.

The coil assembly started at the central plane by piling up the prefabricated racetrack layers on a provisional surface. Care was taken that the upper surface of each layer was at its correct height with respect to the central plane. To achieve this, the wire height was specified slightly below the theoretical height of 3 mm (see Table 2) and, by adding thin fibre-glass strips in between successive layers, the dimension could be corrected. The fibre-glass strips were 0.1 or 0.2 mm thick (selected according to which fitted best) and perforated to permit the passage of helium.

When the first half coil was piled up, the stiffening flange and the coil clamping plates could be fixed. After rotating the whole set-up by 180° around the beam axis, the other half coil was mounted in the same way.

Next, 3 mm thick prefabricated fibre-glass strips were placed in position around the coil, filling in the space between the coil clamping plates so that a roughly cylindrical surface was obtained.

To achieve radial clamping of the coil, 2 mm diameter stainless steel wires were wound around the fibre-glass packing strips and stiffening flanges, passing through grooves machined in the latter. The wires were spaced at 2 cm intervals and stressed at a tension of 100 kg. With this tension still on the wire, the ends were spot-welded together to form a ring. In Fig. 7 (and also in Fig. 10), a part of the coil can be seen with the tightening wires in position.

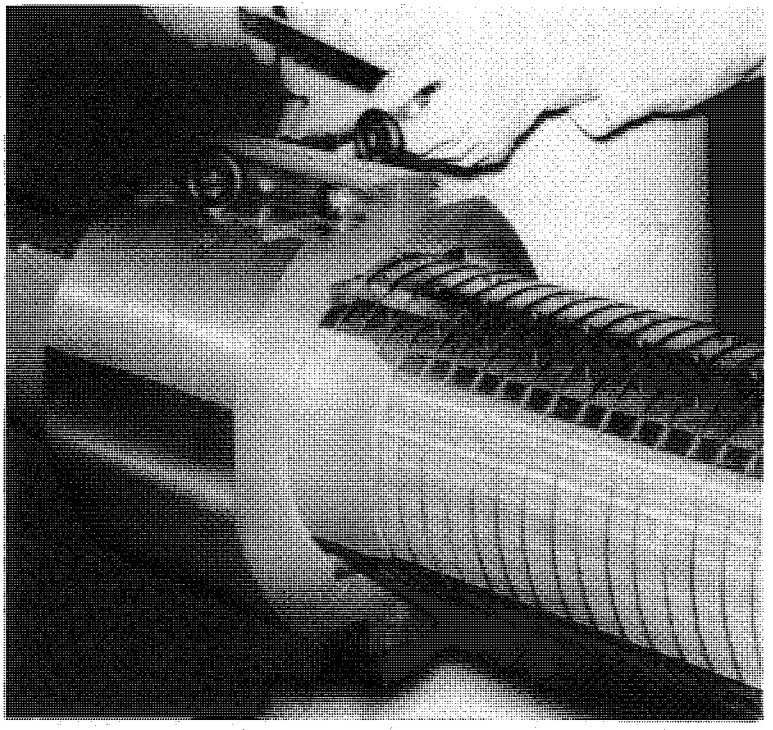

Fig. 7 Moulding the smooth cylindrical surface

The last preparation before mounting the magnetic iron rings was to prepare a smooth cylindrical surface, well centred with respect to the axis of the magnet, with the same radius as the inner surface of the iron rings. This was achieved by moulding epoxy putty (Ciba XD 580) on the outer fibre-glass surface using a precisely machined and located mould (Fig. 7). The width of the mould made it possible to cover a length of 12 cm at a time. It was teflon-coated to facilitate demoulding. The resin, readily mixed with the hardener, was applied on the outer surface of the fibre-glass strips in the form of "sausages", the volume of which was slightly greater than the volume of the space to be filled. Then the resin was squeezed out by tightening the mould against the stiffening flanges, on which it was centred by appropriate stops. After a setting time of one hour, the mould could be taken off and the same procedure started again. The surface quality thus obtained was excellent, and a perfect fit to the inner iron surface resulted from it.

3.5 Iron assembly

The forged magnetic iron, the magnetic properties of which are indicated in Table 4, were machined in the form of half rings as shown in Fig. 3a. The thickness of each half ring is 8 cm, and 27 pairs are needed to cover the length of one magnet. The total weight of the iron shield of each magnet is 1500 kg.

Table 4

Properties of the magnetic iron

Magnetic field strength	2000	5000	21000	A/m
Magnetic induction (min.)	1.6	1.72	2.0	T
Remanence max. 0.9 T Coercive force max. 150 A/m				

The rings were positioned (Fig. 8), starting at the centre of the magnet, with a 0.15 mm space between adjacent rings. When the magnet is cold this space reduces to approximately 0.07 mm because of the differential shrinkage between the coil assemblies and the iron. There is also a vertical gap between the iron half rings, allowing the tightening of the clamping bolts to a given torque in order to obtain the desired amount of pre-stress.

In addition to acting as a magnetic shield, the iron also serves to transmit the electromagnetic forces to the clamping bolts. Without taking into account the attraction between

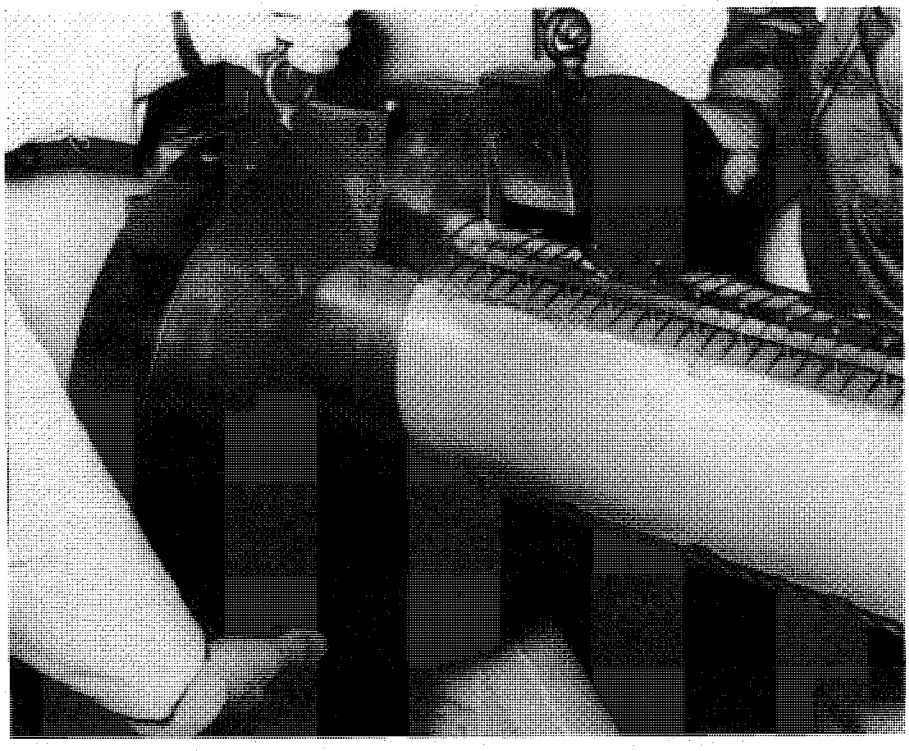

Fig. 8 Positioning the iron rings

the iron half rings, these forces would be around 1 ton per cm of magnet length. With the M 16 bolts used, this force results in a stress of approximately 15 kg/mm^2. The invar sleeves serve to keep the coil under pre-stress during cooldown, when the inner section shrinks slightly more than the magnetic iron.

After tightening the nuts of the clamping bolts with a torque wrench, the gaps in between all pairs of half rings differed only by a few tenths of a millimetre.

3.6 Coil end assembly

The way in which the coil ends are assembled may be understood best by looking at Fig. 9. The vertical end of each layer is separated from its adjacent layers by a 3 mm thick fibre-glass packing piece. Another fibre-glass plate with a cut-out of the shape of the layer end surrounds the layer itself. In this way, the whole coil end is filled with packing, resulting in an approximately cubic shape. It is apparent that such a shape was easy to clamp by means of coil end clamping bolts (see Fig. 3b). There are some vertical grooves in the fibre-glass packing plates to allow the helium to circulate.

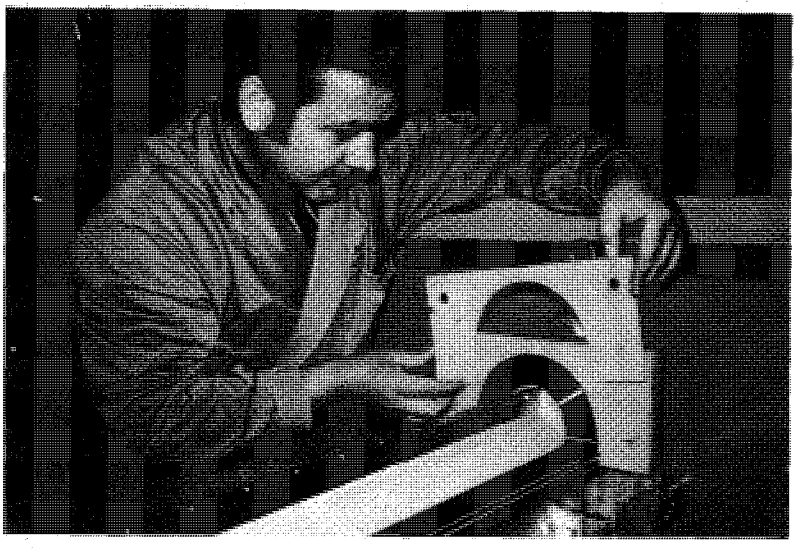

Fig. 9 Assembly of the coil ends

On one of the coil ends, the layers had to be electrically interconnected in series. Figure 10 shows how at an earlier stage of the assembly the wire ends of each layer, with the insulation already stripped and the surface covered with an indium film, protruded from the coil end. Each wire was then bent down flat onto the surface and the terminal wire of the adjacent layer was indium-soldered on top of it (Fig. 11). A typical resistance achieved with this method is $2 \times 10^{-9}\ \Omega$ *), which means that the total extra heat developed by the 40 internal connections is less than 50 mW at the nominal current.

---

*) The authors are grateful to Dr. R. Wolf, CERN ISR Division, for having carried out a series of measurements to study the contact resistance.

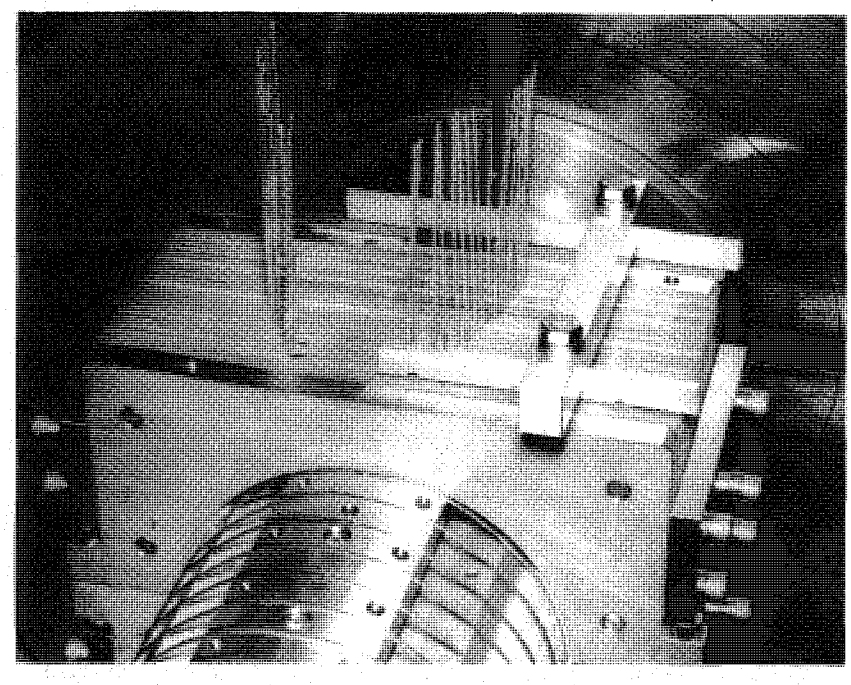

Fig. 10 Coil end ready for inter-layer connection

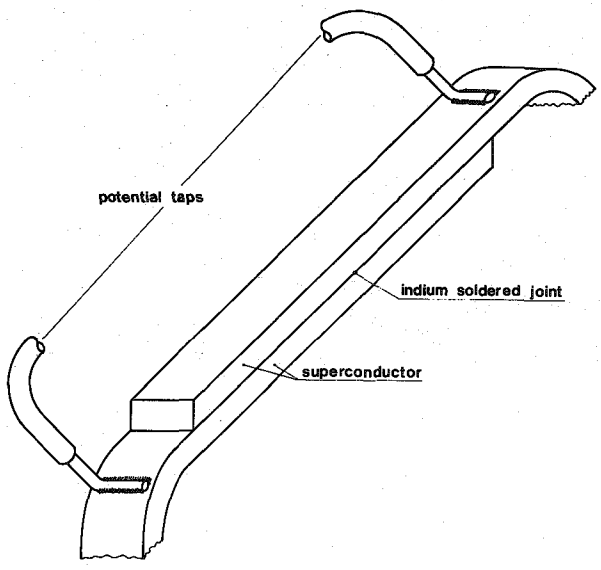

Fig. 11 Detail of inter-layer connection

The soldered joints are clamped down with a cover plate, perforated to allow the passage of helium, as shown in Fig. 12, which presents the coil end completely assembled. A pair of potential taps is connected to each soldered joint to allow a resistance check. The end connections of the whole coil are joined to gold-plated copper bars on the end of the magnet. The wires seen rolled up on the side of the magnet are thermocouples.

Figure 13 shows the entire magnet.

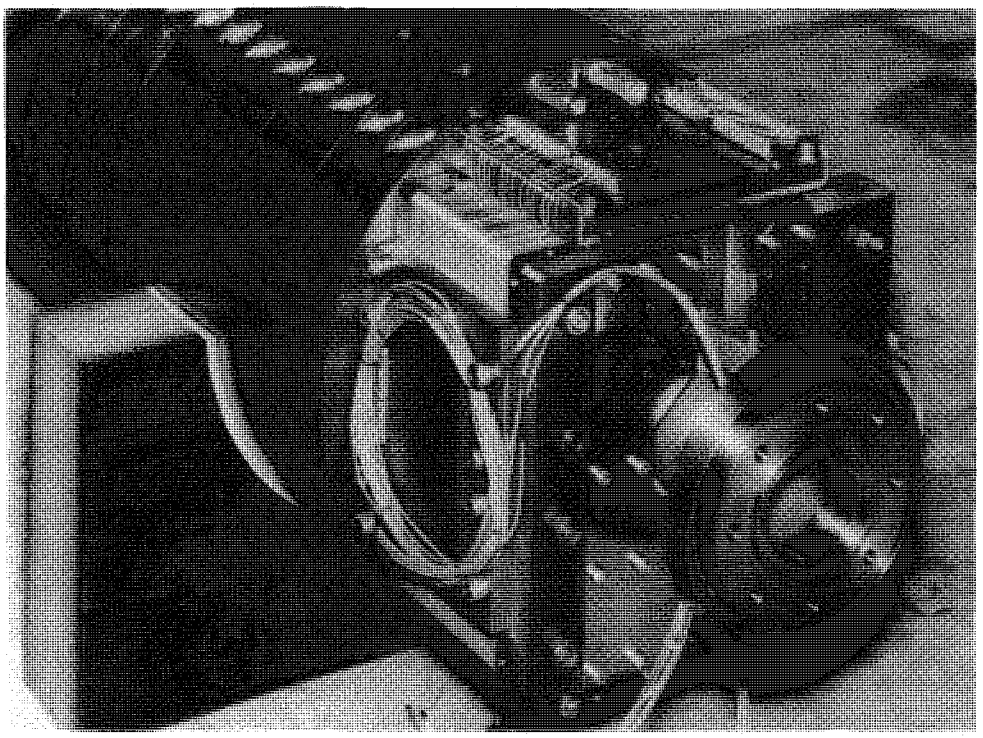

Fig. 12 Coil end completely assembled

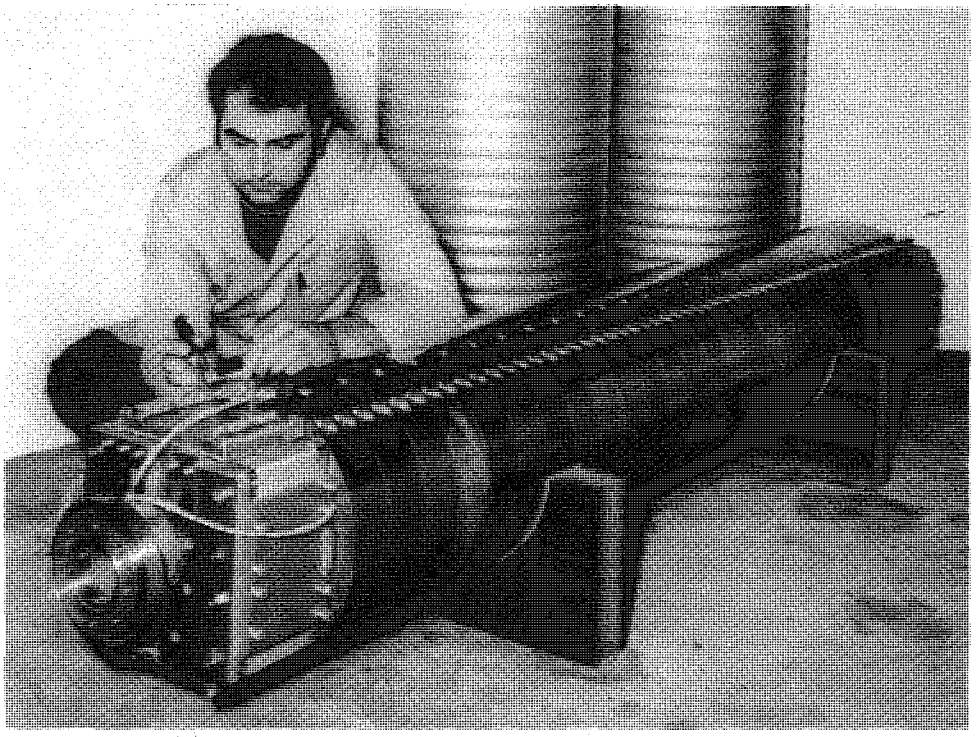

Fig. 13 Magnet completely assembled

4. MAGNET TEST IN VERTICAL CRYOSTAT

Once the magnets had reached the state as shown in Fig. 13 they were tested in a provisional vertical cryostat. The reason for this was that the final cryostat is an entirely welded construction, so that the risk of mounting an un-tested magnet in it was considered too high.

The training history of both magnets was rather different (Fig. 14). SBM II quenched for the first time at 95% of the nominal current and the average increase was then 12 A per quench. The training of SBM III started at 83% of the nominal current, and the current then rose by only 4 A per quench on the average. No explanation was found for this difference, but since the magnets are identical, with the exception of the conductor, it is supposed that the conductor used in SBM III is, for reasons not yet clearly understood, less stable than that of SBM II.

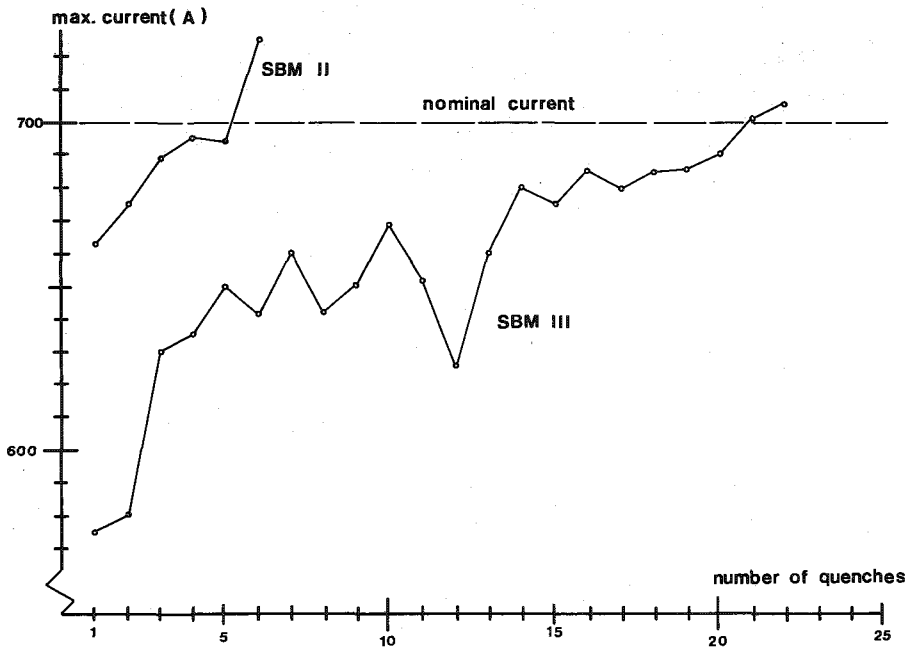

Fig. 14 Training curves; current versus number of quenches

In spite of some difficulties in measuring the contact resistance of the indium-soldered joints between the layers because of noise problems, it was nevertheless ascertained that none of them exceeded a resistance of about 10^{-9} Ω, which was well within the expected range.

After warm-up to room temperature, all clamping bolts of the iron shielding were retightened, as some of them were found to be slightly loose.

5. CRYOSTAT DESIGN

5.1 General

As can be seen from Fig. 15, the magnet cryostat consists in principle of the following concentric elements:

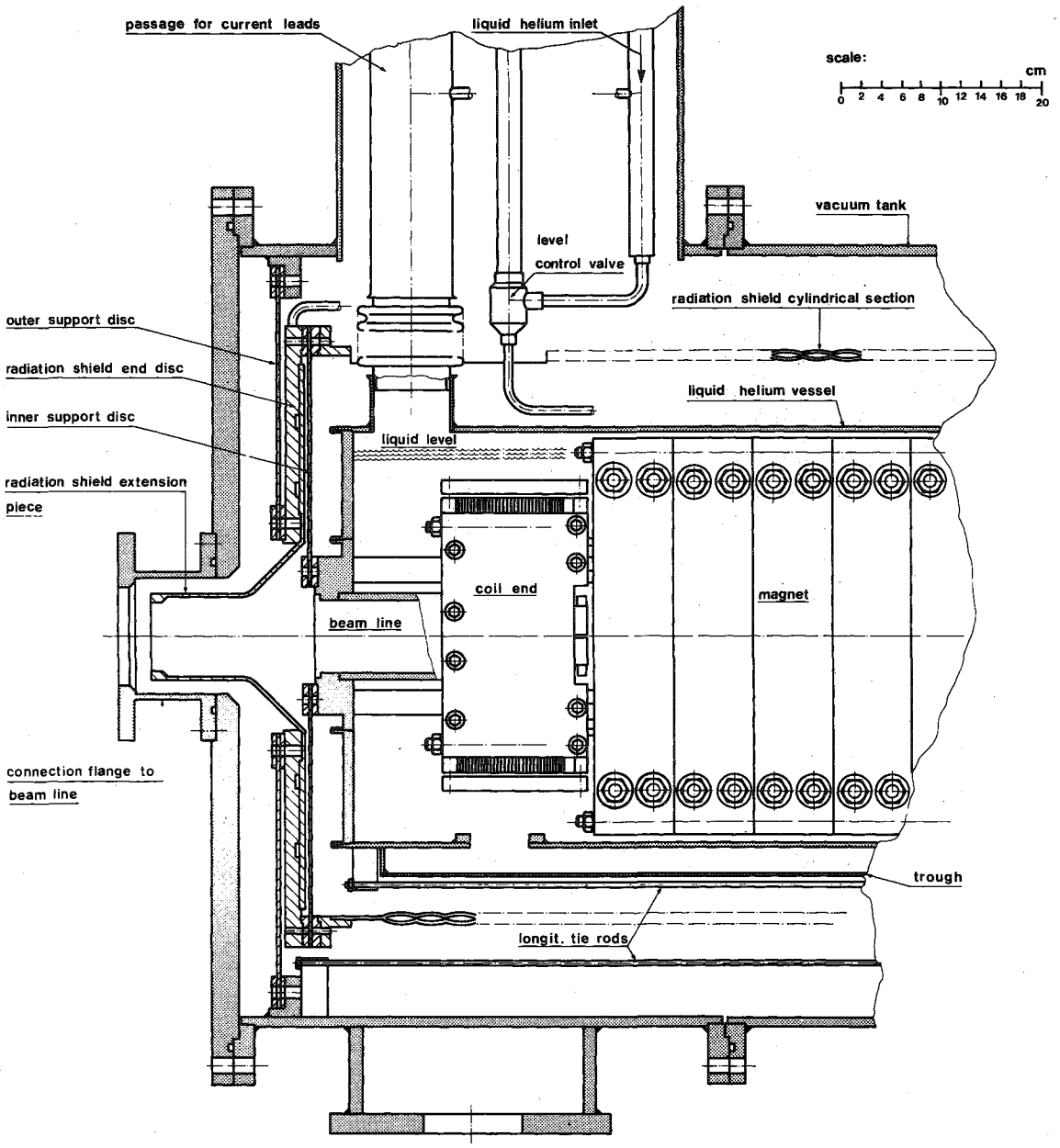

Fig. 15 Typical longitudinal cross-section through cryostat end

- the inner liquid helium vessel containing the magnet;
- the gas-cooled radiation shield;
- the vacuum tank;
- the suspension system at either end, each system consisting of three disks and an extension piece.

Figure 16 shows the main parts of the cryostat during a trial assembly. Table 5 gives the main dimensions of the cryostat elements.

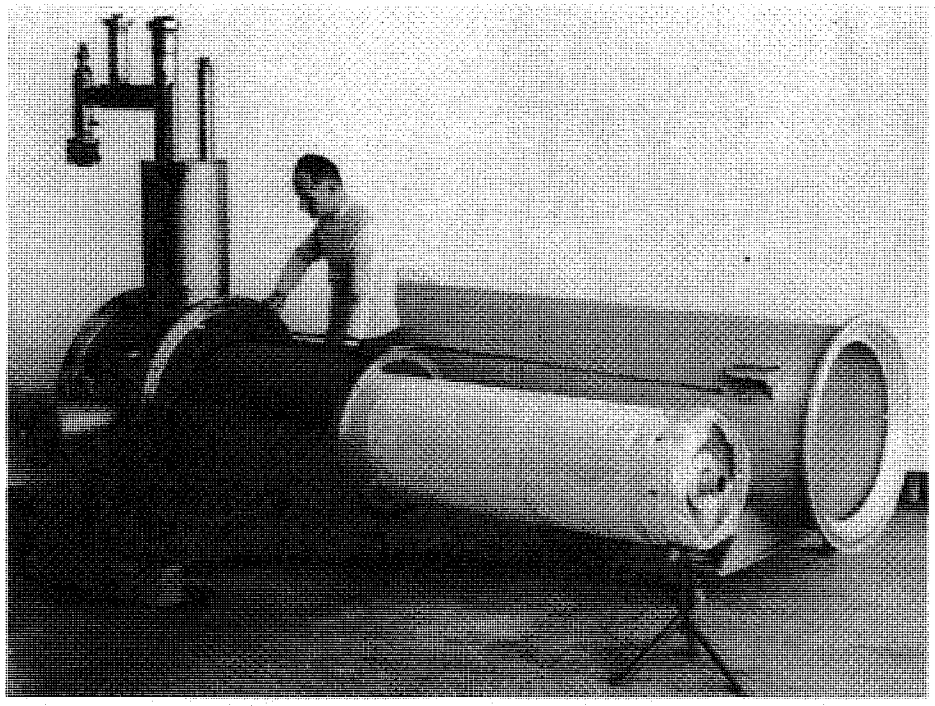

Fig. 16 Trial assembly showing super-insulated helium vessel, radiation shield, and vacuum tank

Table 5

Dimensions of cryostat elements

Liquid vessel inner diameter	408 mm
Liquid vessel length	2642 mm
Cold magnet bore diameter	74 mm
Radiation shield diameter	570 mm
Radiation shield length incl. extensions	2782 mm
Vacuum vessel outside diameter	790 mm
Vacuum vessel length over flanges	2800 mm
Total magnet length incl. gate valves	3150 mm
Total magnet weight	3.5 tons

5.2 The liquid helium vessel

The all stainless steel liquid helium vessel has an inner diameter of 408 mm and a net liquid volume of about 50 litres (i.e. with the magnet in place). In order to avoid the inherent danger of inaccessible cold joints, the vessel was entirely welded up once the magnet had been installed and all electrical connections made.

A trough on the bottom of the liquid vessel (see Figs. 3a and 15) is a special feature to facilitate the cooldown of the magnet to liquid nitrogen temperature. The procedure is

the following: liquid nitrogen from a slightly pressurized dewar is connected to the liquid inlet, so that the flow can be controlled by the liquid filling valve. The tube from this valve to the liquid vessel enters the trough at the bottom; consequently a liquid level can be established and automatically controlled inside the trough without the liquid being in contact with the magnet itself. An electrical heater brazed on the outer surface of the trough can now be powered, producing a corresponding flow of cold gas, the level in the trough being kept constant by an automatic level control system.

The flow of cold gas which enters the cylindrical vessel through a row of holes is then directed along the annular space between the vessel and the magnet thus providing efficient cooling. The gas passes through the radiation shield before leaving the magnet. The cool-down speed may be varied by adjusting the heating power. It was generally set to approximately 2°/hour; the maximum temperature difference measured within the magnet during cool-down was then 18°.

5.3 The radiation shield

The radiation shield is cooled by a partial stream of helium boil-off gas. The shield consists of two end disks and a cylindrical section. The end disks, which also serve as a load-bearing part of the suspension system, are made from thick stainless steel disks into which a spiral groove has been machined. A flat circular copper plate is brazed to each disk thus forming a channel for the flow of the helium boil-off gas. In addition, this plate is extended by a funnel-shaped copper piece which reduces the angle of heat radiation into the cold beam bore.

The cylindrical section is made from thin stainless-steel plate and uses the hollow wall principle to provide a series of annular passages which are connected in series with the flow through the end disks.

Aluminized mylar superinsulation is provided between the liquid vessel and the radiation shield as well as between the radiation shield and the vacuum tank.

5.4 The vacuum tank

The vacuum tank is composed of two cylindrical sections and two end flanges. The shorter section, being equipped with feedthroughs to the liquid vessel, gas outlets, and the vacuum pumping stud, is made of stainless steel for ease of welding. All other parts are made of aluminium alloy. Tightness is provided by O-ring joints.

The connection from the vacuum tank to the beam line needs some attention. Most beam lines are evacuated, but the vacuum is in general poor, so that a separation had to be foreseen at the magnet ends. A 0.2 mm thick mylar window is used for this purpose. However, as a safety precaution, gate valves have been provided on each connection flange to the beam line; these valves close automatically should a mylar window rupture. They would always be closed should it be necessary to disconnect a magnet. The small volumes between the mylar windows and the gate valves can be evacuated separately.

In this particular case the three cryostats have a common vacuum, and mylar windows are installed only at the beam entry and exit of the whole system.

5.5 The suspension system

The outer and the inner disk of the suspension system are made of fibre-glass, 2 mm thick, with stainless steel flanges glued to them to reinforce the fixation. A third disk in between the two fibre-glass disks is made of copper and stainless steel and forms the radiation shield end disk, as was explained in Section 5.3.

All heat entering through the outer disk by solid conduction is removed by cold gas, circulating in the radiation shield end disk. Consequently, the only heat flow arriving at the liquid by solid conduction is caused by the temperature gradient between the radiation shield and the liquid vessel along the inner fibre-glass disk. This heat flow is however small, as the radiation shield temperature can easily be kept at around 50 K, even with a moderate gas flow.

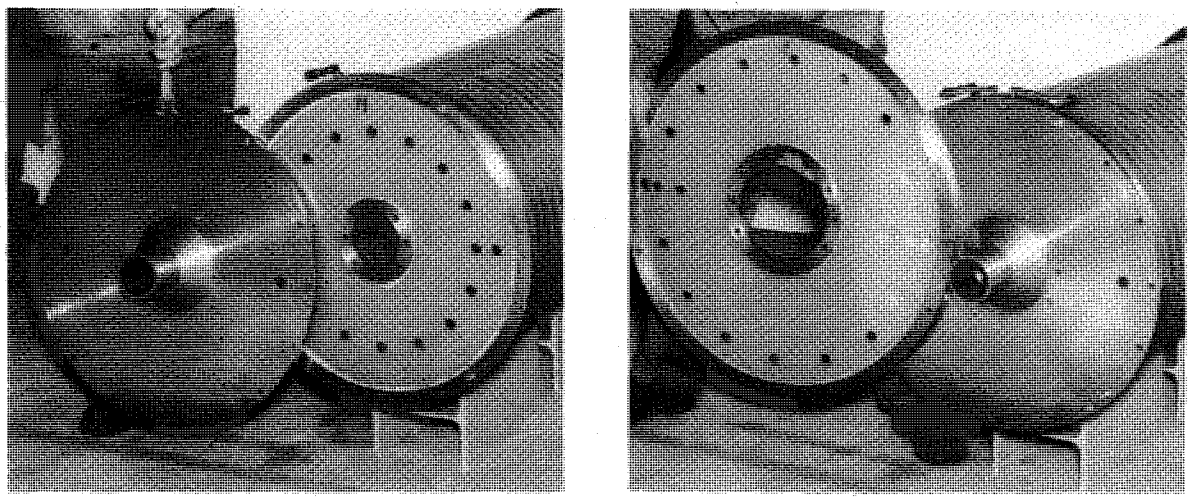

a) b)

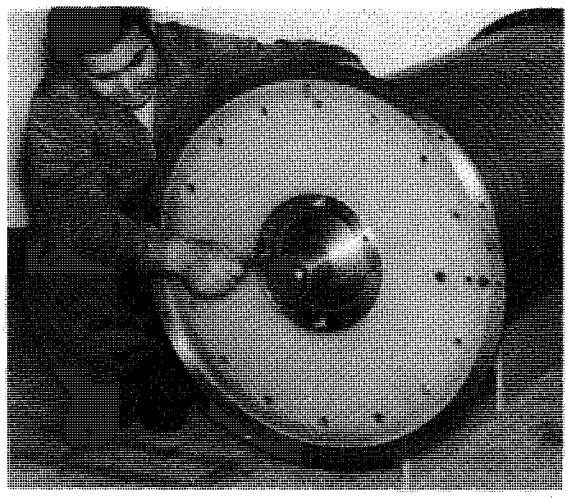

c)

Fig. 17 Trial assembly of suspension system

When designing this type of support, it seemed wise to test the strength of a fibre-glass disk under realistic conditions. The exact replica of a disk mounted on a test rig was loaded up to 5 tons, while the outer circumference remained at room temperature and the inner circumference was cooled to liquid nitrogen temperature. The disk did not fail nor did it show any deterioration after warm-up. Since the load is only about 1.5 ton per suspension system, the disk design was considered safe.

An advantage of this kind of suspension system is that because of its axial symmetry no displacement of the magnet axis takes place during cooldown. The longitudinal differential shrinkage of the inner vessel and the radiation shield with respect to the vacuum tank is easily absorbed by a slight conical deformation of the fibre-glass disks. There is, however, a possibility for the whole inner part of the magnet to oscillate horizontally along the beam axis. To prevent this, longitudinal tie rods are mounted as shown in Fig. 15.

Figures Fig. 17a to 17c show how the elements of the suspension system were put together during a trial assembly.

6. CURRENT LEADS

Current leads must be carefully designed from the point of view of thermal losses, but they must also be sufficiently safeguarded against accidental overheating.

In this particular case, they had to be sectionally small for space reasons. The solution chosen is shown in Fig. 18. The leads consist, in principle, of two square copper bars, 10 × 10 mm^2, into which zig-zag grooves are machined on two opposite sides. The grooves provide the necessary passages for the helium counterflow cooling. The triangular prisms which remain between the grooves hardly participate in the current conduction, but owing to their mass they keep the thermal time-constant of the lead high. Consequently, even if the cooling gas flow is entirely stopped, the increase of temperature is slow enough to discharge the magnet safely.

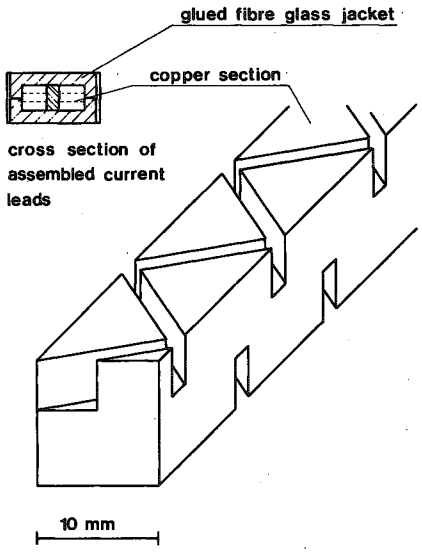

Fig. 18 Detail of current lead

The two leads, separated by a 2 mm thick fibre-glass strip, are then enclosed in a fibre-glass jacket, the two halves of which are glued together. The bottom connection to the superconductor is indium-soldered and immersed in the helium bath.

The characteristics of the leads were studied in a test cryostat. The losses at minimum cooling (i.e. with the cooling gas flow adjusted so that the temperature of the outcoming gas was at room temperature) were approximately 1.3 mW/A at a current of 750 A.

7. FLOW SCHEME AND INSTRUMENTATION

The magnets are required to operate over extended periods with a minimum of supervision. A certain number of automatic control circuits were therefore necessary, but an attempt was made to keep the system as simple as possible.

Figure 19 shows a simplified flow scheme of one magnet. The pressures in the supply dewar and in the magnet are kept constant, so that a fixed pressure difference, typically 50 g/cm^2, is available for the transfer. The filling valve is actuated by a proportional controller which in turn receives a signal from a superconducting level gauge.

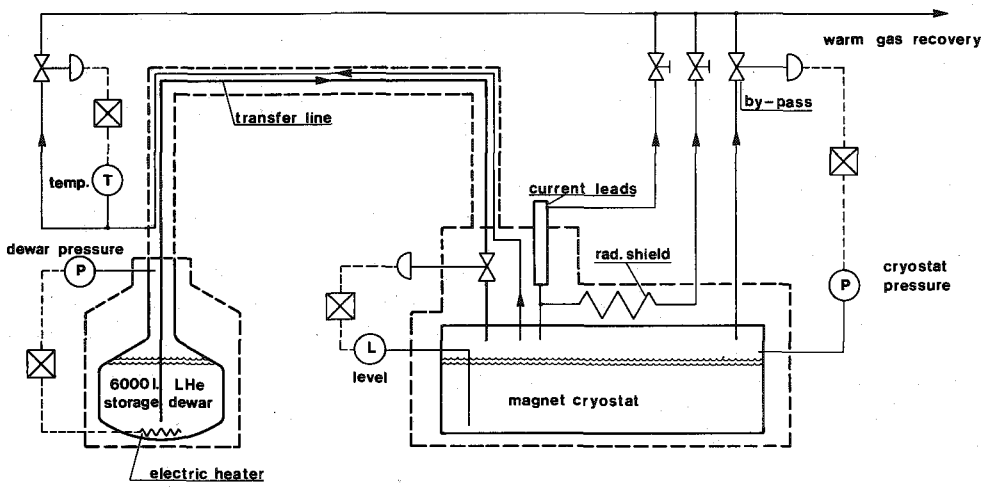

Fig. 19 *Simplified helium flow scheme*

There are four gas outlets from the magnet:

i) The flow of cold gas through the magnet radiation shield. This is set to a value ensuring sufficiently low temperatures along the shield, measured by several thermocouples.

ii) The flow through the radiation shield of the supply transfer line. This is controlled in such a way that the temperature at the gas outlet of the transfer line remains constant.

iii) The cooling gas flow through the current leads. A fixed flow is set irrespective of the current to provide static cooling, to which is added a flow proportional to the voltage drop along the current leads to avoid overheating when the magnet is charged.

iv) The flow through a by-pass valve, operated in such a way that the pressure in the magnet cryostat is kept constant.

Some electric instrumentation is also required. Besides the level control already mentioned, the voltage between the upper and the lower half coil of the magnet is compared and, if there is a significant difference, the power supply is switched off, thus discharging the magnet. The same happens if the voltage across the current leads exceeds a certain value (danger of overheating) or if the helium level drops below the minimum level. The power supply is stabilized to 10^{-4} (long term) by means of a transistor bank in series with the load. The outer protection circuit for the magnet consists of a series of high current diodes.

8. MAGNET PERFORMANCE

Before cooling SBM II in its final horizontal cryostat (Fig. 20), two calibrated pick-up coils*) were inserted in the beam tube for magnetic measurements. Both pick-up coils were 1 cm wide and 3 m long, i.e. they exceeded the length of the magnet coil at either end by 30 cm. They were both positioned in the horizontal magnet symmetry plane, one in the magnet centre, the other on the edge of the free bore almost touching the beam tube, 30 mm apart from the centre line. By integrating the induced voltage during a charge cycle, the field integral $\int B \cdot d\ell$ of the magnet could be measured as well as the difference of this value along the two lines at which the pick-up coils were positioned.

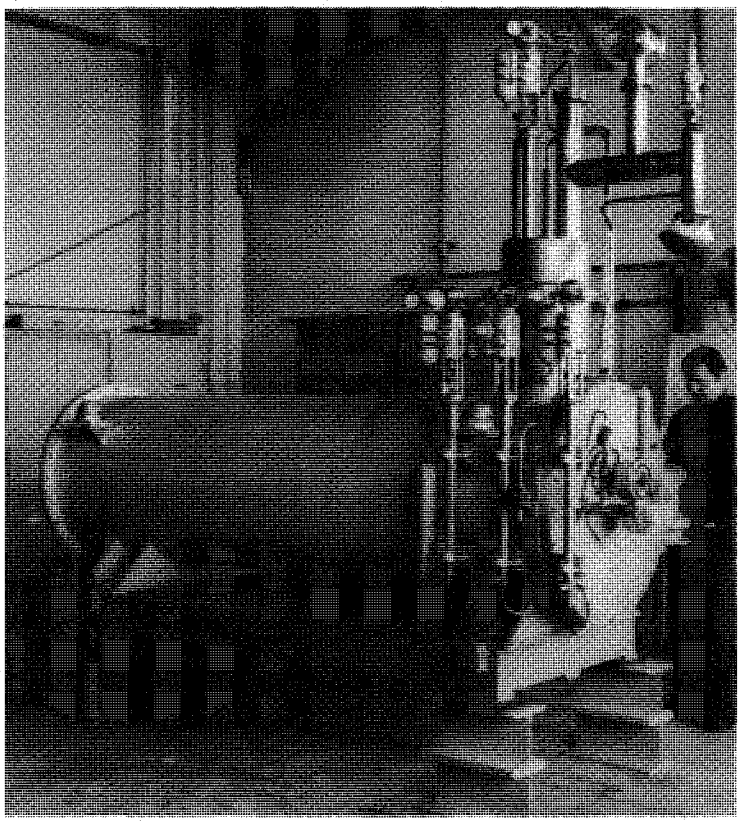

Fig. 20 Completed magnet cryostat

*) The authors wish to thank Mr. V. Hatton, CERN SPS Division, for manufacturing of the pick-up coils, and Mr. D. Lehm, EP Division, for their calibration.

Figure 21 shows the calibration curve of SBM II obtained in this way, and the field integral difference between the central and the outer pick-up coil. Since the measured curve ended up near the calculated point, the computation was assumed correct and no further magnetic measurements were made.

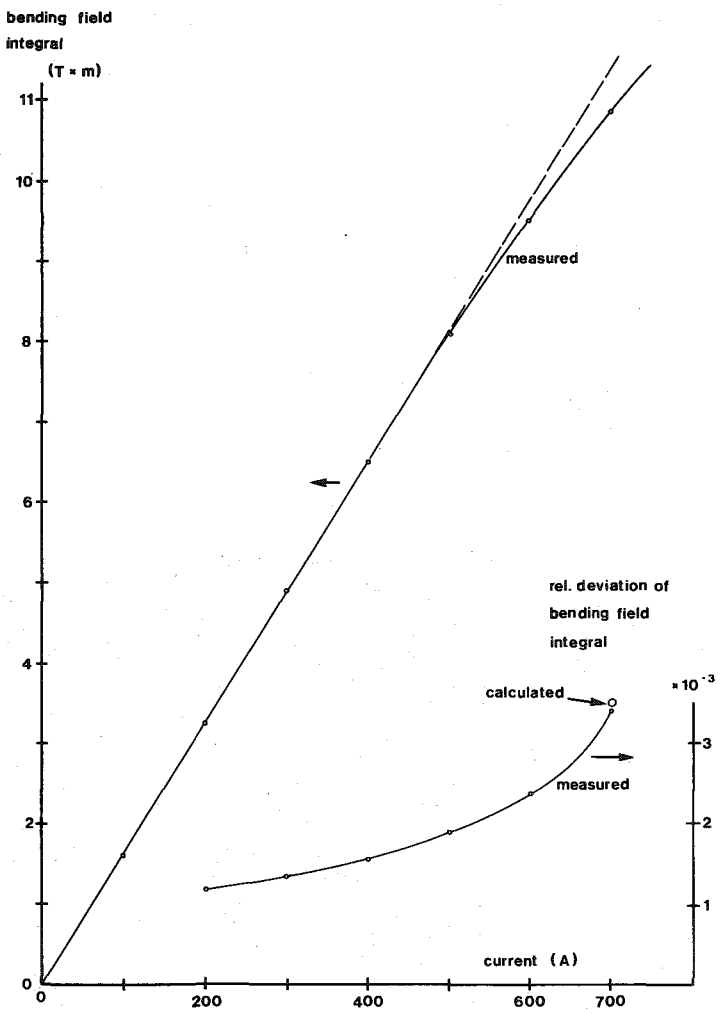

Fig. 21 Magnet calibration curve and field integral inhomogeneity versus current

SBM II quenched at 715 A, i.e. 10 A below the last quench in the vertical test cryostat, after which it was operated in the s_3 beam for about one year at currents up to 670 A without quenching again.

Since the results obtained with SBM II were as predicted, no magnetic measurements were made with SBM III. After mounting in its horizontal cryostat, this magnet was immediately installed and used in the beam at currents up to 670 A without quenching.

The cryogenic losses of the two magnets are identical and amount to approximately 4 W per magnet at full current, not taking into account the transfer losses, which are of the order of 2 W per magnet.

Acknowledgements

The construction of the magnets described was essentially the work of a small group consisting of D. Guyon (instrumentation), G. Fersurella and the late G. Janon (coil winding and magnet assembly), and P. Le Cossec (cryostat assembly and tests).

For the magnet tests and the installation in the beam, valuable support was given by our colleagues of the Low Temperature Laboratory, B. Chamdru, M. Firth, R. Frachet and A. Juillerat.

The high quality of the work performed in several CERN workshops also largely contributed to the good results obtained.

* * *

REFERENCES

1) CERN Courier, Vol. 13 (1973), p. 144.

2) H. Brechna and P. Turowski, Proc. 6th Internat. Conf. on Magnet Technology, Bratislava, 1977 (to be published).

3) H. Desportes, Proc. 5th Internat. Conf. on Magnet Technology, Rome, 1975 (Lab. Naz. CNEN, Frascati, 1975), p. 502.

4) Ch. Iselin, CERN Computer Program Library No. T 600.

5) W. Müller and W. Wolff, ETZ-A, Vol. 94 (1973), p. 276.

6) D. Evans, J.T. Morgan and G.B. Stapleton, Rutherford Laboratory RHEL/R 251 (1972).